

SUPPLEMENTARY ONLINE DATA

Inter- and intra-molecular interactions of *Arabidopsis thaliana* DELLA protein RGL1

David J. SHEERIN*†, Jeremy BUCHANAN*, Chris KIRK*†, Dawn HARVEY†, Xiaolin SUN†, Julian SPAGNUOLO*, Sheng LI‡, Tong LIU‡, Virgil A. WOODS‡, Toshi FOSTER†, William T. JONES†¹ and Jasna RAKONJAC*†

*Institute of Molecular Biosciences, Massey University, Private Bag 11 222, Palmerston North, New Zealand, †The New Zealand Institute for Plant and Food Research Limited, Private Bag 11 030, Palmerston North, New Zealand, and ‡Department of Medicine, University of California San Diego, La Jolla, CA, U.S.A.

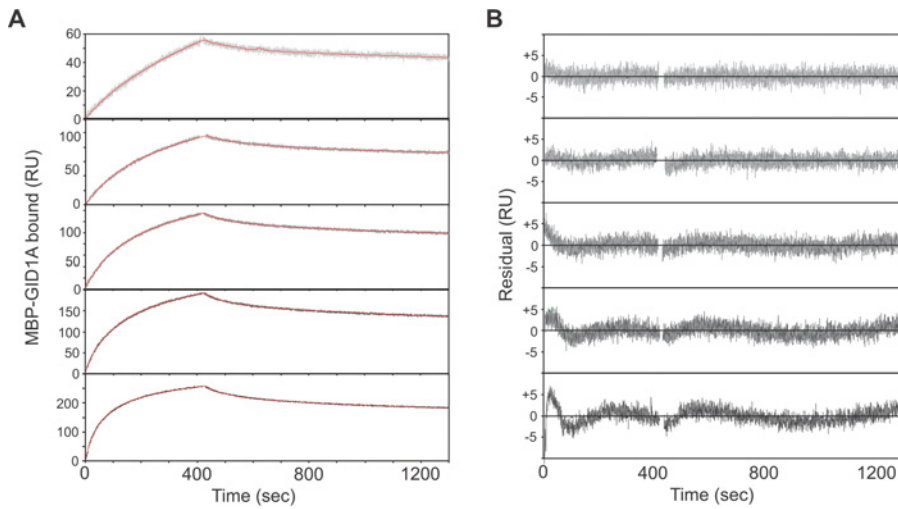


Figure S1 Conformational change kinetic modelling of the gibberellin-dependent GID1A–RGL1N interaction

(A) Gibberellin-dependent association and dissociation data for the interaction between GID1A and immobilized RGL1^N, detected by SPR. Interactions were performed for 100, 200, 400, 800 and 1600 nM solutions of GID1A (top to bottom). A calculated two-state kinetic model was fitted to individual curves, indicated in red, using BiaEvaluation software version 3.1. (B) Residual plot for variance in response units (RU), of the kinetic data from the calculated model for each GID1A concentration.

¹ Correspondence may be addressed to either of these authors (email William.Jones@plantandfood.co.nz or j.rakonjac@massey.ac.nz).

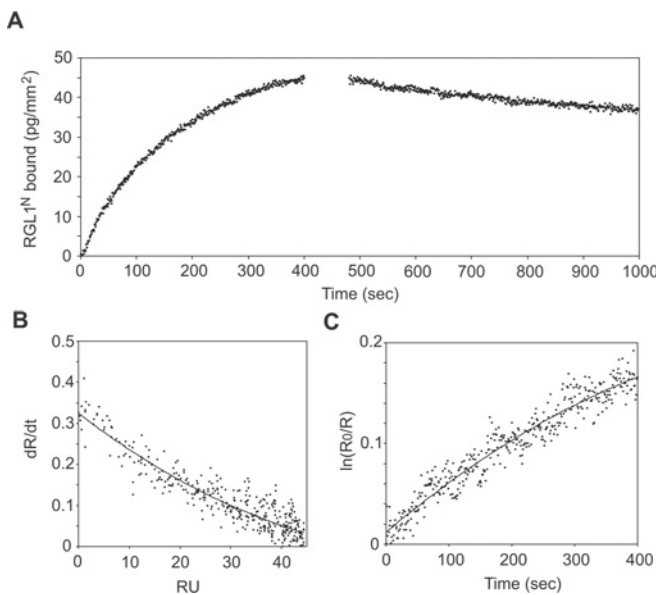


Figure S2 Gibberellin-dependent binding of RGL1^N to immobilized GID1A

(A) Predicted RGL1^N (residues 1–137) tertiary structure, modelled from the GID1A/GA4:GA1^{11–113} crystal structure using SwissModel (PDB code 2ZSI) [2,3]. Conserved residues that form direct interactions between GAI and GID1A [2] are shown in blue. (B–D) RGL1^N model, indicating monoclonal antibody epitopes: 6C8 (B), BC9 (C) and AD7 (D). Antibody epitopes are highlighted in red and yellow. Yellow indicates a residue that also forms a direct GAI–GID1A interaction, whereas red residues do not.

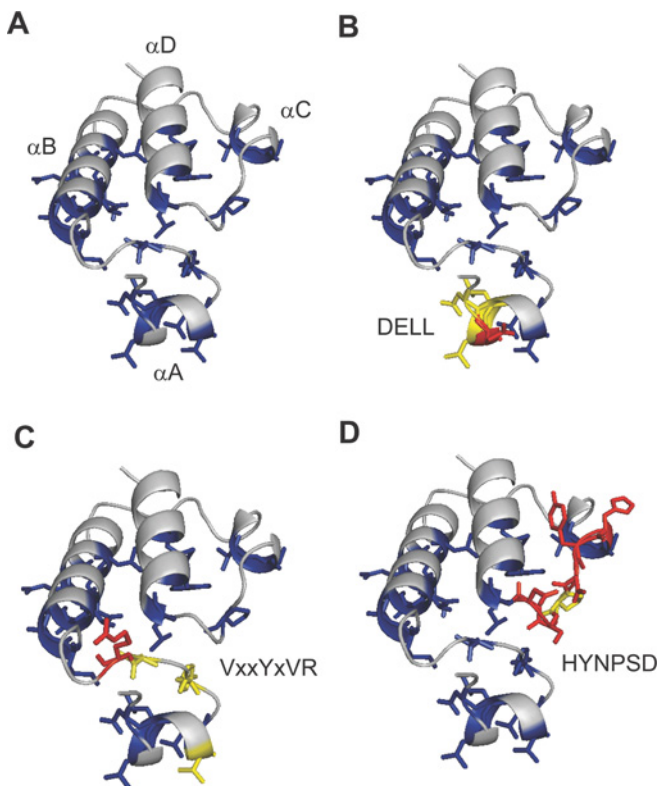


Figure S3 Structural prediction of the RGL1 N-terminal DELLA domain when in complex with GID1A

(A) Predicted RGL1^N (residues 1–137) tertiary structure, modelled from the GID1A/GA4:GA1^{11–113} crystal structure using SwissModel (PDB code 2ZSI) [2,3]. Conserved residues that form direct interactions between GAI and GID1A [2] are shown in blue. (B–D) RGL1^N model, indicating monoclonal antibody epitopes: 6C8 (B), BC9 (C) and AD7 (D). Antibody epitopes are highlighted in red and yellow. Yellow indicates a residue that also forms a direct GAI–GID1A interaction, whereas red residues do not.

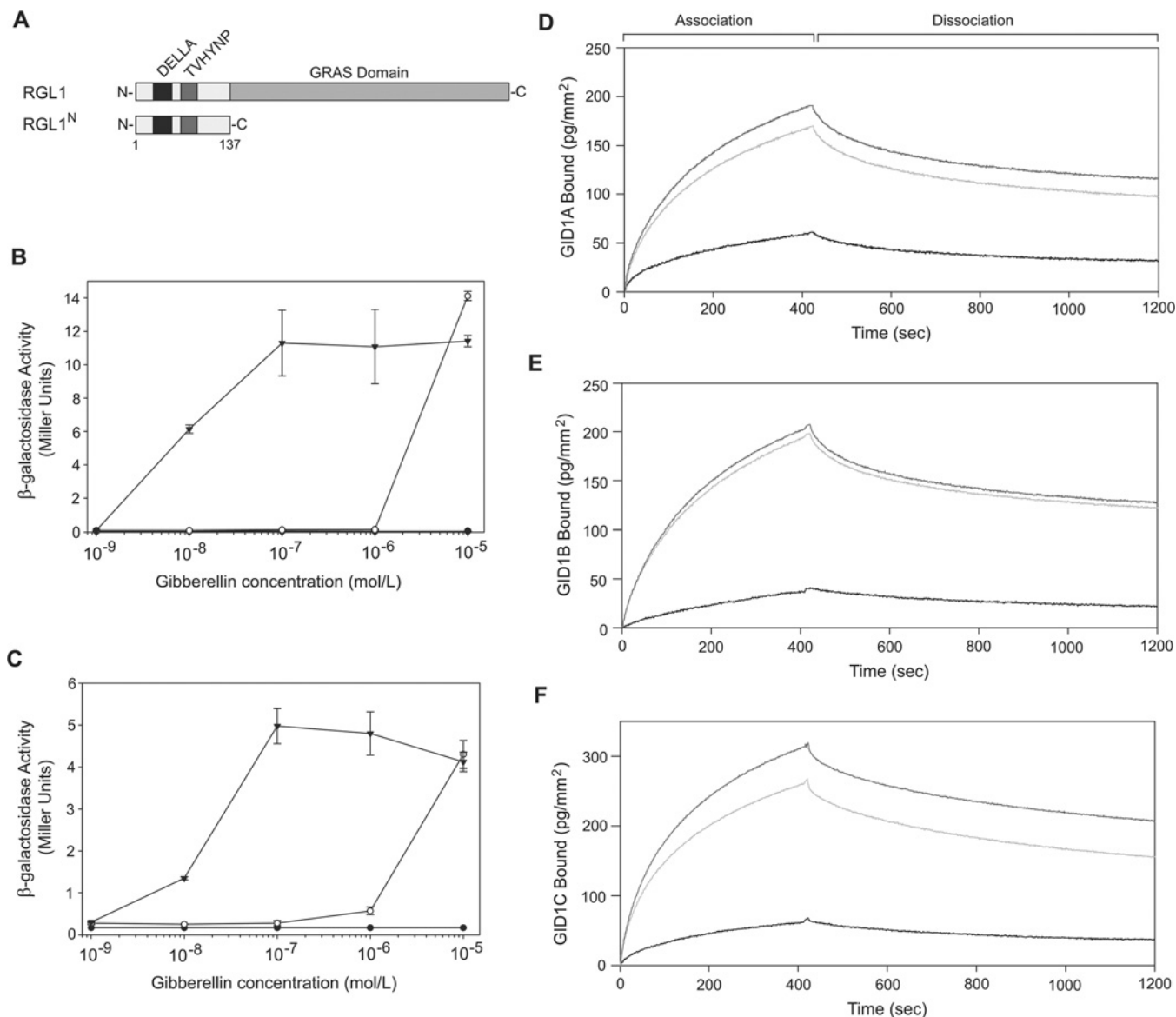


Figure S4 Comparison of the GA₃- and GA₄-dependent GID1A-RGL1^c interaction *in vivo* and *in vitro*

(A) Schematic representation of RGL1, and the N-terminal 137 residues of RGL1, RGL1^N, used in *in vitro* experiments. (B) and (C) Dose-response curves of yeast two- and three-hybrid assays. (B) Two-hybrid assay of the interaction between the Gal4 DNA-binding domain fusion of GID1A and the Gal4 activation-domain fusion of RGL1. (C) Three-hybrid assay of the interaction between the Gal4 DNA-binding domain fusion of SLY1 and the Gal4 activation domain fusion of RGL1 in the presence of GID1A. LacZ (β -galactosidase) reporter gene activity, from *Saccharomyces cerevisiae* grown in absence of gibberellins ([EPS]) and the presence of GA₃ ([EPS]) or GA₄ ([EPS]). The experiment was performed in duplicate (from two independent transformants); β -galactosidase assays were performed in triplicate for each transformant. Error bars show ± 1 S.D. (D–F) *In vitro* association and dissociation of gibberellin-saturated GID1A-C and RGL1^N; monitored using SPR. Interaction of RGL1^N with: (D) GID1A, (E) GID1B or (F) GID1C; in the absence (black), or presence of 100 M GA₃ (light grey) or 100 M GA₄ (dark grey). Gibberellins were mixed with GID1A-C 30 min prior to the binding assay and excluded from running buffer during the dissociation phase. Association, 0–420 s; dissociation, 420–1200 s. The amount of bound GID1A-C is shown as pg/mm² of surface area.

**Figure S5** DELLA protein alignment

The full-length sequences for DELLA proteins from a range of plant species were aligned using AlignX (Vector NTI software, Invitrogen). Absolutely conserved residues are highlighted in orange; highly conserved residues are highlighted in blue; highly similar residues are highlighted in green; and similar residues are highlighted in yellow. The RGL1 gain-of-function mutants used in the present paper are displayed. The sequences of several DELLA gain-of-function mutations are also displayed, indicating in-frame deletions or amino acid replacements. The *A. thaliana* (At) *gai-1*, *rga^{A17}*; grape (*Vv, Vitis vinifera*) *gai-1*; (*Zm, Zea mays*) rice (*Os, Oryza sativa*) *slrlw^{ΔDELLA}*, *slrl^{ΔSPACE}*, *slrl^{ΔTVHYNP}*, *slrl^{ΔS/T/V}*; barley (*Hv, Hordeum vulgare*) *sln1-d*; wheat (*Ta, Triticum aestivum*) *rht*, *rht-B1b*, *rht-D1b*; and maize field mustard (*Br, Brassica rapa*) *rga1-d*; *d8-MP* have been previously described as semi-dominant gibberellin-insensitive mutations [4–11]. Ps, pea (*Pisum sativum*).

**Figure S5 Continued**

**Figure S5 Continued**

Table S1 Oligonucleotide sequences for amplification and sequencing

Description	Sequence
RGL1 forward primer for pACT2 (XmaI)	5'-TCCCCGGGTATGAAGAGAGAGCACAACCAC-3'
RGL1 reverse primer for pACT2 (Sacl)	5'-CGAGCTCGTTACCCACACGATTGATTGCC-3'
RGL1 internal nt93 reverse primer	5'-GACGTGGCACACAAGCTG-3'
RGL1 internal nt145 forward primer	5'-CACTCCGGCAGCTCTTC-3'
RGL1 internal nt213 reverse primer	5'-AGCATGCTCTGGATCTTGAC-3'
RGL1 internal nt268 forward primer	5'-ATTGAGATTCCATCCAAGAAC-3'
RGL1 internal mutagenic primer reverse	5'-CTTGATTGAGCTCTTGCTTAC-3'
RGL1 internal nt830 forward primer	5'-CCGGCCATTGTAACCATGG-3'
RGL1 internal nt411 reverse primer	5'-GTCCTCTCCCTTACTCATCCGCACCCGTAGAGGATAACTCCGAT-3'
RGL1 internal nt412 forward primer	5'-GATGGATGAACATACAAAGGAGGGTCGCTCTGTTGGTTGGATT-3'
RGL1 forward for pMalc2x (BamHI)	5'-CGGATCCATGAAGAGAGCACAACCAC-3'
RGL1 reverse N-term internal for pMalc2x (Sall)	5'-GACGCGTCGACTTAGAGGATAACTCCGATTCAA-3'
GID1A forward primer for pGBK77 (EcoRI)	5'-GGAATTATGGCTGCGAGCGATGAAG-3'
GID1A reverse primer for pGBK77 (BamHI)	5'-CGGGATCCGTTAACATCCGCGTTACAAAC-3'
GID1A forward primer for pBridge MCSII (NotI)	5'-ATAAGAATGCGGCCGCTATGGCTGCGAGCGATGAAG-3'
GID1A reverse primer for pBridge MCSII (NotI)	5'-ATAAGAATGCGGCCGCTATTAAACATTCCCGTTACAAAC-3'
GID1B forward primer for pGBK77 (EcoRI)	5'-GGAATTATGGCTGCTGTTACGAAGT-3'
GID1B reverse primer for pGBK77 (BamHI)	5'-CGGGATCCGCTAAGGAGTAAGAAGCAGG-3'
GID1C forward primer for pGBK77 (EcoRI)	5'-GGAATTATGGCTGAAAGTGAAGAAGT-3'
GID1C reverse primer for pGBK77 (BamHI)	5'-CGGATCCGTTATGGCATTCTCGCTTAC-3'
SLY1 forward primer (EcoRI)	5'-CGGATCCGTTATGGGATCTGGAAAGAGGTC-3'
SLY1 reverse primer (BamHI)	5'-CGGGATCCGTTATGGGATCTGGAAAGAGGTCCTTAGTGAAACTCATCTCTTAG-3'
GFP forward primer	5'-ATCGGAGTTACCTCTACGGGTGGCAATGAGTAAAGGAGAAGAAC-3'
GFP reverse primer	5'-GATCCAAACACACAGAGCGACCCCTCCCTTGATAGTCATCCAGC-3'
pACT2 forward sequencing primer	5'-CTATCTATTGATGATGAAGATAC-3'
pACT2 reverse sequencing primer	5'-AGTTGAAGTGAACCTGCGGGTT-3'
pGBK77 forward sequencing primer (T7)	5'-TAATACGACTCACTATAGGG-3'
pGBK77 / pBridge MCSII reverse sequencing primer	5'-TAAGAGTCACTTAAATTGTAT-3'
pBridge MCSII forward sequencing primer	5'-TGGGGAACTGTGGTGGTTG-3'
pBridge MCSII reverse sequencing primer	5'-CCGTATTACCCCTTGAGT-3'
pGADT7 forward sequencing primer	5'-TAATACGACTCACTATAGGG-3'
pGADT7 reverse sequencing primer	5'-GTGAACCTGCGGGTTTCAGTATCTACGATT-3'
pMALc2x forward sequencing primer	5'-GGTCGTCAGACTGTCGATGAAGCC-3'
pMALc2x reverse sequencing primer	5'-CGCCAGGGTTCCAGTCACGAC-3'

REFERENCES

- 1 Sun, X. L., Frearson, N., Kirk, C., Jones, W. T., Harvey, D., Rakonjac, J., Foster, T. and Al-Samarrai, T. (2008) An *E. coli* expression system optimized for DELLA proteins. Protein Expression Purif. **58**, 168–174
- 2 Murase, K., Hirano, Y., Sun, T. P. and Hakoshima, T. (2008) Gibberellin-induced DELLA recognition by the gibberellin receptor GID1. Nature **456**, 459–463
- 3 Arnold, K., Bordoli, L., Kopp, J. and Schwede, T. (2006) The SWISS-MODEL workspace: a web-based environment for protein structure homology modelling. Bioinformatics **22**, 195–201
- 4 Peng, J. R., Carol, P., Richards, D. E., King, K. E., Cowling, R. J., Murphy, G. P. and Harberd, N. P. (1997) The *Arabidopsis* GAI gene defines a signaling pathway that negatively regulates gibberellin responses. Genes Dev. **11**, 3194–3205
- 5 Peng, J. R., Richards, D. E., Hartley, N. M., Murphy, G. P., Devos, K. M., Flintham, J. E., Beales, J., Fish, L. J., Worland, A. J., Pelica, F. et al. (1999) 'Green revolution' genes encode mutant gibberellin response modulators. Nature **400**, 256–261
- 6 Itoh, H., Ueguchi-Tanaka, M., Sato, Y., Ashikari, M. and Matsuoka, M. (2002) The gibberellin signaling pathway is regulated by the appearance and disappearance of SLENDER RICE1 in nuclei. Plant Cell **14**, 57–70
- 7 Muangprom, A., Thomas, S. G., Sun, T. P. and Osborn, T. C. (2005) A novel dwarfing mutation in a green revolution gene from *Brassica rapa*. Plant Physiol. **137**, 931–938
- 8 Hirano, K., Asano, K., Tsuji, H., Kawamura, M., Mori, H., Kitano, H., Ueguchi-Tanaka, M. and Matsuoka, M. (2010) Characterization of the molecular mechanism underlying gibberellin perception complex formation in rice. Plant Cell **22**, 2680–2696
- 9 Boss, P. K. and Thomas, M. R. (2002) Association of dwarfism and floral induction with a grape 'green revolution' mutation. Nature **416**, 847–850
- 10 Chandler, P. M., Marion-Poll, A., Ellis, M. and Gubler, F. (2002) Mutants at the *Slender* locus of barley cv Himalaya: molecular and physiological characterization. Plant Physiol. **129**, 181–190
- 11 Weston, D. E., Elliott, R. C., Lester, D. R., Rameau, C., Reid, J. B., Murfet, I. C. and Ross, J. J. (2008) The pea DELLA proteins LA and CRY are important regulators of gibberellin synthesis and root growth. Plant Physiol. **147**, 199–205

Received 23 November 2010/19 January 2011; accepted 15 February 2011
 Published as BJ Immediate Publication 15 February 2011, doi:10.1042/BJ20101941